View Article Online
View Journal

Dalton Transactions

An international journal of inorganic chemistry

Accepted Manuscript

This article can be cited before page numbers have been issued, to do this please use: S. Dutta, P. Bhunia, J. Mayans, M. Drew and A. Ghosh, *Dalton Trans.*, 2020, DOI: 10.1039/D0DT00952K.

ROYAL SOCIETY OF CHEMISTRY

rsc.li/dalton

Roles of basicity and steric crowding of anionic coligands in catechol oxidase like activity of Cu(II)-Mn(II) Complexes

Sabarni Dutta[a], Pradip Bhunia[a], Júlia Mayans[b], Michael G. B. Drew[c], Ashutosh Ghosh[a,*]

[a]*Department of Chemistry, University College of Science, University of Calcutta, 92, A.P.C. Road, Kolkata 700 009, India, E-mail address: ghosh_59@yahoo.com*

[b]*Departament de Química Inorgànica I Orgànica, Secció Inorgànica and Institut de Nanosciència I Nanotecnologia (IN^{2}UB). Martíi Franqués 1-11. 08028, Barcelona, Spain.*

[c]*School of Chemistry, The University of Reading, P.O. Box 224, Whiteknights, Reading RG6 6AD, UK.*

Abstract

Five new heterometallic Cu(II)-Mn(II) discrete trinuclear complexes, $[(CuL)_2Mn(CH_3COO)_2]$ (**1**), $[(CuL)_2Mn(NO_3)_2]$ (**2**), $[(CuL)_2Mn(C_6H_5COO)(H_2O)]Cl$ (**3**), $[(CuL)_2Mn((p\text{-}OH)C_6H_5COO)(H_2O)]ClO_4$ (**4**) and $[(CuL)_2Mn(HCOO)(H_2O)]ClO_4$ (**5**) have been synthesized using a metalloligand, CuL derived from an N_2O_2 donor Schiff base, H_2L (*N*,*N*′-bis(α-methylsalicylidene)-1,3-propanediamine). Single-crystal structural analyses reveal that all five complexes have a common $[(CuL)_2Mn]$ core, where two terminal metalloligands, CuL are connected to the central metal ion, Mn(II) *via* double phenoxido bridges. Among the complexes, **1** and **2** possess linear structures where the terminal Cu(II) atoms are bridged to the central Mn(II) atoms by acetate and nitrate ions, respectively along with the double phenoxido bridges whereas **3**, **4** and **5** have bent structures in which the respective anionic co-ligands, benzoate, *p*-hydroxybenzoate and formate ions are coordinated only to central Mn(II) in monodentate fashion along with a water molecule that complete its hexa-coordinated geometry. Among the complexes, **1**, **3**, **4** and **5** show quite high bio-mimicking catecholase like activity for the aerial oxidation of 3,5-di-*tert*-butylcatechol with turnover numbers (k_{cat}) of 139 h^{-1}, 439 h^{-1}, 348 h^{-1} and 730 h^{-1}, respectively whereas complex **2** is practically inactive towards this reaction. The presence of the coordinated water molecule to Mn(II) in the bent complexes, **3**−**5**, appears to be responsible for their high catalytic activity and the difference in their activity may be attributed to steric crowding due to the anionic co-ligand whereas the inactivity of **2** seems to be associated with the low basicity of the nitrate ion. The temperature-dependent dc molar magnetic susceptibility measurements reveal that complexes **1**−**5** are antiferromagnetically coupled with the exchange coupling constants (J) = –8.54 cm^{-1}, –11.50

cm^{-1}, –19.83 cm^{-1}, –10.65cm^{-1} and –10.27 cm^{-1} for **1**, **2**, **3**, **4** and **5** respectively as is expected from the Cu−O−Mn bridging angles.

Introduction

Synthesis and characteristic study of heterometallic complexes with N, O donor ligands have been a point of interest in the field of coordination chemistry for a long time. This is predominantly because of their potential applications in catalytic, magnetic, gas storing and sensing activities.[1] A plethora of heterometallic Schiff base complexes has been reported in the past with various types of N, O donor ligands; of which Robson-type macrocycles, bi-compartmental N_2O_4 donor ligands or mono-compartmental N_2O_2 donor ligands deserve special mention.[2] The easy synthetic pathways, involving generally one-pot condensation of a diamine with two salicylaldehyde derivatives and their exceptional complexing ability, boost the popularity of such Schiff base ligands. Recently many Cu(II) complexes of N_2O_2 donor Schiff base ligands have been used as 'metalloligands' to react with various 3d/4f metal salts for the synthesis of heterometallic complexes.[3] The anionic part of such metal salts not only balance the charge of the resultant complex but also plays a crucial role in modulating the nuclearity and structures of these heterometallic complexes *via* different modes of coordination to the metal centres.[4] These anion dependent structural variations are very important in understanding the intriguing structural factors that govern the magnetic properties and catalytic activities of the complexes.[5]

The magnetic coupling of oxo bridged homometallic complexes have been studied extensively and the magneto-structural correlations of these complexes are now well-established.[6] However, such correlations for 3d-3d' hetero-metallic complexes are not that well documented as these complexes are relatively rare.[7] The N_2O_4 donor Schiff bases have been used frequently for synthesis of heterometallic complexes but these rigid ligands allow only little variations in the bridging angle. On the other hand, the trinuclear complexes of N_2O_2 donor Schiff base ligands, synthesised by metalloligand approach are quite flexible and the bridging angles in these complexes can be varied in a wide range by changing the anionic co-ligands.[4] Moreover, heterometallic coordination complexes can show interesting magnetic properties since the combination of different spins in a single cluster generates more magnetic anisotropy.[8]

One of the most promising applications of these heterometallic complexes is in the field of catalysis. Homometallic coordination complexes of 3d metal ions, Cu(II), Ni(II), Co(II/III), Mn(II/III), and Fe(II/III) were used as model catalysts for oxidase type reactions.[9] Among them the catalytic properties of Cu(II) complexes were studied extensively since many naturally occurring metalloproteins like

View Article Online
DOI: 10.1039/D0DT00952K

cytochrome *c* oxidase, catechol oxidase, phenoxazinone synthase *etc*., have copper ions in their active sites.[10] However, the catalytic efficiency of these model complexes is significantly less than that of the native biological enzymes. Therefore, improvement of the catalytic efficiencies of these complexes is a great challenge and with this aim several modifications were made in the coordination environment of the closely knit metal ions. Recently, it is found that heterometallic complexes containing Mn(II) ions catalyse such oxidation reactions.[11] It has also been observed that a coordinated solvent molecule at the Mn(II) center considerably enhances the catalytic oxidase activity in comparison to a Mn(II) centre without the coordinated solvent. Detailed mechanistic study suggested that the presence of labile solvent molecule enhance substrate-catalyst binding as it can be replaced easily by the substrate, which in turn increases the efficiency of the catalyst. However, till date no study has been performed to investigate whether the anionic coligands which are invariably a part of this kind of trinuclear complexes, have any effect on the catalytic efficiencies of these complexes.

Herein, we report the synthesis of a series of five complexes, $[(CuL)_2Mn(CH_3COO)_2]$ (**1**), $[(CuL)_2Mn(NO_3)_2]$ (**2**), $[(CuL)_2Mn(C_6H_5COO)(H_2O)]Cl$ (**3**), $[(CuL)_2Mn((p\text{-}OH)C_6H_5COO)(H_2O)]ClO_4$ (**4**) and $[(CuL)_2Mn(HCOO)(H_2O)]ClO_4$ (**5**) and their characterization by single crystal X-ray diffraction. Complexes **1** and **2** are isostructural having linear geometry being bridged by acetate/nitrate co-anions while complexes **3**, **4** and **5** possess bent structures with a water molecule coordinated to the central Mn(II) atom. The temperature dependent dc magnetic susceptibility measurements reveal antiferromagnetic interactions between the Cu(II) and Mn(II) centers in all five complexes. The coupling constants of the complexes fit well in the magnetostructural correlations of similar phenoxido bridged Cu(II)-Mn(II) complexes. Apart from complex **2**, all the other complexes show catalytic activities towards catechol oxidase activities. The difference in catalytic activity of the isostructural complexes **1** and **2** has been explained in terms of the basicity of the respective anionic co-ligands acetate and nitrate. However the prominent differences in the k_{cat} values of **3**−**5** can be correlated to the effect of steric crowding on catalytic activities. ESI-mass spectra have been used to get an idea about the probable intermediates of these catalytic oxidation reactions and thus a possible mechanism is proposed.

Experimental Section

Starting materials

2-hydroxyacetophenone, 1,3-propanediamine and *p*-hydroxybenzoic acid were purchased from Spectrochem India and formic and benzoic acid from Lancaster Synthesis. All the chemicals were of reagent grade and commercially available. They were used for reactions without further purification.

Caution! Although not encountered during experiment, perchlorate salts of metal complexes with organic ligands are potentially explosive. Only a small amount of material should be prepared and it should be handled with care.

Synthesis of Schiff base ligand (H_2L) and the "metalloligand" (CuL)

The Schiff base ligand, H_2L and its corresponding copper metalloligand (CuL) have been prepared following the reported method.[12] To account briefly, a 20 mL methanolic solution of 2-hydroxyacetophenone (10 mmol, 1.206 mL) and 1,3-propanediammine (5 mmol, 0.420 mL) was refluxed for 2 h. The yellow coloured ligand solution so obtained was cooled, and a methanolic solution of $Cu(ClO_4)_2 \cdot 6H_2O$ (1.852 g, 5 mmol, 10 mL) was added to it with stirring. Triethylamine (1.4 mL, 10 mmol) was then added to this solution and stirring was continued for 20 min. The brown solution thus obtained was filtered and kept in an open atmosphere for slow evaporation of the solvent. Brownish green crystals of the precursor metalloligand were collected by filtration after two days.

Synthesis of the complexes $[(CuL)_2Mn(CH_3COO)_2]$ (1) and $[(CuL)_2Mn(NO_3)_2]_2$ (2)

Methanolic solutions of $Mn(CH_3COO)_2 \cdot 4H_2O$ (0.245 g, 1 mmol) and $Mn(NO_3)_2 \cdot 4H_2O$ (0.251 g, 2 mL, 1 mmol) were mixed with methanolic solutions of the metalloligand, CuL (0.772 g, 5 mL, 2 mmol) for complexes **1** and **2** respectively. The mixtures were well stirred and then filtered. Dark green coloured filtered solutions were carefully layered with diethylether in long tubes for slow diffusion. Deep green rod shaped crystals of **1** and light green needle shaped crystals of **2** appeared at the junction of the two solutions within a few days.

Complex 1: Yield 0.688 g (75%). $C_{42}H_{46}Cu_2MnN_4O_8$ (916.87). Calculated: C, 54.90; H, 5.27; N, 6.10; Cu, 13.83; Mn, 5.98; found: C, 54.87; H, 5.30; N, 6.12; Cu, 13.68; Mn, 5.82. IR (KBr): $\nu_{s+as}(COO^-)$ = 1583, 1541, 1383 cm^{-1}, $\nu(C=N)$ = 1599 cm^{-1}.

Complex 2: Yield 1.351 g (68%) (with respect to CuL). $C_{82}H_{101}Cu_4Mn_2N_{12}O_{23}$ (1986.83). Calculated: C, 49.46; H, 4.37; N, 9.11; Cu, 13.77; Mn, 5.95 found: C, 49.42; H, 4.40; N, 9.09; Cu, 13.91; Mn, 5.78. IR (KBr): $\nu(NO_3^-)$ = 1293 cm^{-1}, $\nu(C=N)$ = 1599 cm^{-1}.

Synthesis of the complex $[(CuL)_2Mn(C_6H_5COO)(H_2O)]Cl$ (3)

To a methanolic solution of CuL (0.772 g, 5 mL, 2 mmol), a methanolic solution of $MnCl_2 \cdot 4H_2O$ (0.197 g, 1 mmol) was added and stirred well. A methanolic solution of benzoic acid (0.122 g, 1 mmol, 5 mL) was added to this solution followed by triethylamine (138 µL, 1 mmol) and mixed well by stirring. The

resulting solution was layered with diethylether carefully in a long layer tube. Light green X-ray quality single crystals started to appear at the junction of the two solutions within two days. We could not prepare X-ray quality single crystals using $Mn(ClO_4)_2 \cdot 6H_2O$ salt hence we used $MnCl_2 \cdot 4H_2O$ instead.

Complex 3: Yield 1.469 g (75%) (with respect to CuL). $C_{90}H_{90}Cl_2Cu_4Mn_2N_8O_{15}$ (1958.68). Calculated: C, 59.88; H, 5.03; N, 5.37; Cu, 13.55; Mn, 5.86; found: C, 59.86; H, 4.97; N, 5.35; Cu, 13.43; Mn, 5.71. IR (KBr): $\nu_{s+as}(COO^-)$ = 1579, 1540, 1398 cm^{-1}, ν(C=N) = 1602 cm^{-1}.

Synthesis of the complexes $[(CuL)_2Mn((p\text{-}OH)C_6H_5COO)(H_2O)]ClO_4$ (4) and $[(CuL)_2Mn(HCOO)(H_2O)]ClO_4$ (5)

In case of complexes **4** and **5**, same procedure as reported for complex **3** was followed except for using solid $Mn(ClO_4)_2 \cdot 6H_2O$ (0.330 g, 1 mmol) instead of $MnCl_2 \cdot 4H_2O$. A heterometallic Cu(II)-Mn(II) solution was prepared as before and separate solutions of *p*-hydroxybenzoic acid for **4** (0.138 g, 1 mmol, 5 mL) and formic acid for **5**, in methanol (0.046 g, 1 mmol, 5 mL) were taken and deprotonised using triethylamine (138 µL, 1 mmol). The heterometallic Cu(II)-Mn(II) solutions and the acid solutions were then mixed and filtered. Finally the deep green solutions were layered with diethylether in long tubes for slow diffusion. Light green and deep green X-Ray quality single crystals of complexes **4** and **5** respectively appeared at the junction of two solutions after a few days.

Complex 4: Yield 0.782 g (71%) (with respect to CuL). $C_{45}H_{47}ClCu_2MnN_4O_{15}$ (1101.36). Calculated: C, 56.60; H, 5.07; N, 5.87; Cu, 13.32; Mn, 5.76; found: C, 56.64; H, 5.10; N, 5.85; Cu, 13.54; Mn, 5.92. IR (KBr): $\nu_{s+as}(COO^-)$ = 1583, 1543, 1397 cm^{-1}, ν(C=N) = 1599 cm^{-1}.

Complex 5: Yield 0.586 g (61%) (with respect to CuL). $C_{39}H_{43}ClCu_2MnN_4O_{11}$ (961.26). Calculated: C, 48.73; H, 4.51; N, 5.83; Cu, 14.75; Mn, 6.37; found: C, 48.74; H, 4.53; N, 5.85; Cu, 14.53; Mn, 6.58. IR (KBr): $\nu_{s+as}(COO^-)$ = 1580, 1539, 1384 cm^{-1}, ν(C=N) = 1598 cm^{-1}.

Physical measurements

Elemental analyses (C, H and N) were performed using a PerkinElmer 2400 series II CHN analyzer. IR spectra in KBr pellets (4000–500 cm^{-1}) were recorded using a PerkinElmer RXI FT-IR spectrophotometer. Electronic spectra were measured in a Hitachi U-3501 spectrophotometer for estimation of Cu(II)[13a] and Mn(II)[13b], employing the 'neo-cuproin' and periodate methods, respectively. Solid-state, variable-temperature and variable-field magnetic data were collected on powdered samples using a MPMS5 Quantum Design magnetometer operating at 0.03 T in the 300 to 2.0 K range for the

magnetic susceptibility and at 2.0 K in the 0 to 5 T range for the magnetization measurements. Diamagnetic corrections were applied to the observed susceptibilities using Pascal's constants.

X-ray Crystallography

The structures were solved using direct methods with the Shelxs97 program.[14] The non-hydrogen atoms were refined with anisotropic thermal parameters. The hydrogen atoms bonded to carbon were included in geometric positions and given thermal parameters equivalent to 1.2 times those of the atom to which they were attached. Structure **3** was disordered over a two-fold axis and treated appropriately. The trinuclear moieties in the other structures were ordered although perchlorate anions in **4** and **5** were disordered and solvent molecules were given reduced occupancy. All structures were refined using Shelxl16-6[15] on F^2. Details of the crystallographic data of complexes **1**−**5** are summarized in Table 1. CCDC reference numbers are 1990112−1990116 for complexes **1**−**5** respectively.

Electrochemical measurements.

Electrochemical studies of all five complexes **1**–**5** were performed using a Basi-Epsilon C3 cell instrument at a scan rate of 100 mV s^{-1} within the potential range of 0 to −1.60 V vs. Ag/AgCl and that of CuL at a range of 0 to −1.40 V. Cyclic voltammograms were carried out using 0.1 M TBAP as the supporting electrolyte and 1×10^{-3} M complexes in acetonitrile solution which were deoxygenated by argon purging. The working electrode was a glassy carbon disk (0.32 cm^2) which was polished with alumina solution, washed with absolute acetone and acetonitrile, and air-dried before each electrochemical run. The reference electrode was Ag/AgCl, with platinum as the counter electrode. All experiments were performed in standard electrochemical cells at 25 °C.

Table 1. Crystal data and structure refinement of complexes **1**, **2**, **3, 4** and **5**.

Complex	**1**	**2**	**3**	**4**	**5**
Formula	$C_{42}H_{46}Cu_2MnN_4O_8$	$C_{41}H_{50.50}Cu_2MnN_6O_{11.50}$	$C_{45}H_{48}ClCu_2MnN_4O_{7.50}$	$C_{45}H_{53}ClCu_2MnN_4O_{15}$	$C_{40}H_{48}ClCu_2MnN_4O_{12}$
Formula Weight	916.87	1986.83	1958.68	1101.36	995.30
Crystal System	monoclinic	triclinic	monoclinic	monoclinic	monoclinic

Space group	$P2_1/c$	$P\bar{1}$	$C2/c$	$P2_1/c$	Cc
a, Å	10.3064(15)	11.0088(6)	20.3123(6)	15.6553(19)	24.514(2)
b, Å	11.5974(17)	11.5219(7)	14.2566(4)	16.993(2)	10.5637(9)
c, Å	16.442(2)	19.5333(12)	16.4904(5)	19.634(2)	15.9325(14)
α, deg	90	94.180(2)	90	90	90
β, deg	93.429(3)	94.333(2)	95.126(2)	110.755(5)	95.259(3)
γ, deg	90	117.861(2)	90	90	90
V, Å^3	1961.8(5)	2167.7(2)	4756.3(2)	4884.3(10)	4108.5(6)
Z	2	1	2	4	4
ρ_{calc}($g\ cm^{-3}$)	1.552	1.522	1.368	1.498	1.606
μ (Mo Kα) (mm^{-1})	1.451	1.326	1.255	1.242	1.462
F(000)	946	1027	2012	2260	2048
R_{int}	0.058	0.072	0.066	0.139	0.061
Total no. of reflns	43264	51388	26560	81565	19631
No. of unique reflns	3496	7943	4136	9355	7062
No. of rflns with $I>2\sigma(I)$	3192	6447	2879	5060	6396
$R1$,[a] w$R2$[b]	0.0311, 0.0825	0.0649, 0.1736	0.0631, 0.2286	0.0792, 0.2523	0.0486, 0.1247

GOF[c] on F^2	1.11	1.12	1.09	1.05	1.019
$R1$(all)	0.0359	0.0815	0.0932	0.1646	0.0558
Temp, K	296	295	296	295	100
Residual electron density, e $Å^{-3}$	-0.69, 0.27	-0.58, 1.32	-0.38, 1.01	-0.56, 0.91	-0.73, 0.87

[a]$R_1 = \sum||F_o| - |F_c||/\sum|F_o|$, [b]$wR_2$ $(F_o^2) = [\sum[w(F_o^2 - F_c^2)^2/\sum w\ F_o^4]^{½}$ and [c]GOF $= [\sum[w(F_o^2 - F_c^2)^2/(N_{obs} - N_{params})]^{½}$.

Catalytic Oxidation of 3,5-DTBC.

The catalytic properties of bio-mimicking heterometallic complexes **1**−**5** were examined towards catechol oxidase activity. The catecholase activity involves oxidation of 3,5-di-*tert*-butylcatechol (3,5-DTBC) to 3,5-di-*tert*-butylquinone (3,5-DTBQ). To study this oxidation process, equal volumes of 2 x 10^{-5} M acetonitrile solutions of the complexes were treated with 2 x 10^{-3} M solutions of 3,5-DTBC at room temperature and absorbance *vs*. wavelength scan of the solutions at a range of 300−500 nm were recorded at a regular interval of 3 min for half an hour. 3,5-DTBQ shows a broad absorption peak at 398 nm. The increase of absorbance maxima at 398 nm was also monitored with respect to time (time scan). The formation of hydrogen peroxide as a byproduct of this oxidation process was also detected by iodometric methods as reported previously.[16]

Results and discussion:

Syntheses of the complexes

The tetradentate N_2O_2 donor Schiff base ligand, H_2L was prepared by 1:2 dicondensation of 1,3-propanediamine with 2-hydroxyacetophenone and its Cu(II) complex was prepared as reported earlier.[17] This complex (CuL) has been used as metalloligand for the synthesis of five trinuclear Cu(II)-Mn(II) complexes as shown in Scheme 1. For complexes **1** and **2**, the metalloligand was reacted with $Mn(CH_3COO)_2 \cdot 4H_2O$ and $Mn(NO_3)_2 \cdot 4H_2O$, respectively in 2:1 ratio. For preparation of complexes **3** and **4**, **5**, the metalloligand was first reacted with $MnCl_2 \cdot 4H_2O$ and $Mn(ClO_4) \cdot 6H_2O$ respectively in 2:1 ratio and then these mixtures were treated with corresponding deprotonated acid solution *i.e.*, benzoic

acid for **3**, *p*-hydroxybenzoic acid for **4** and formic acid for **5** in 1:1 molar ratio. The difference in the synthetic procedure results in an interesting difference in the structures and composition of synthesized complexes. In complexes **1** and **2**, two same anionic co-ligands are present per trinuclear unit and both act as bridges between the terminal and central metal ion resulting a linear trinuclear structure; no solvent molecule is coordinated to any of the metal ions. On the other hand, in **3**, **4** and **5** two different type of anions are present; one of them *i.e.*, the carboxylate ion coordinates only to the Mn(II) centre in monodentate mode forming a bent trinuclear structure. A solvent molecule is coordinated to Mn(II) to complete its hexacoordination geometry in each compound. These differences are very important for catecholase like activity of the complexes.

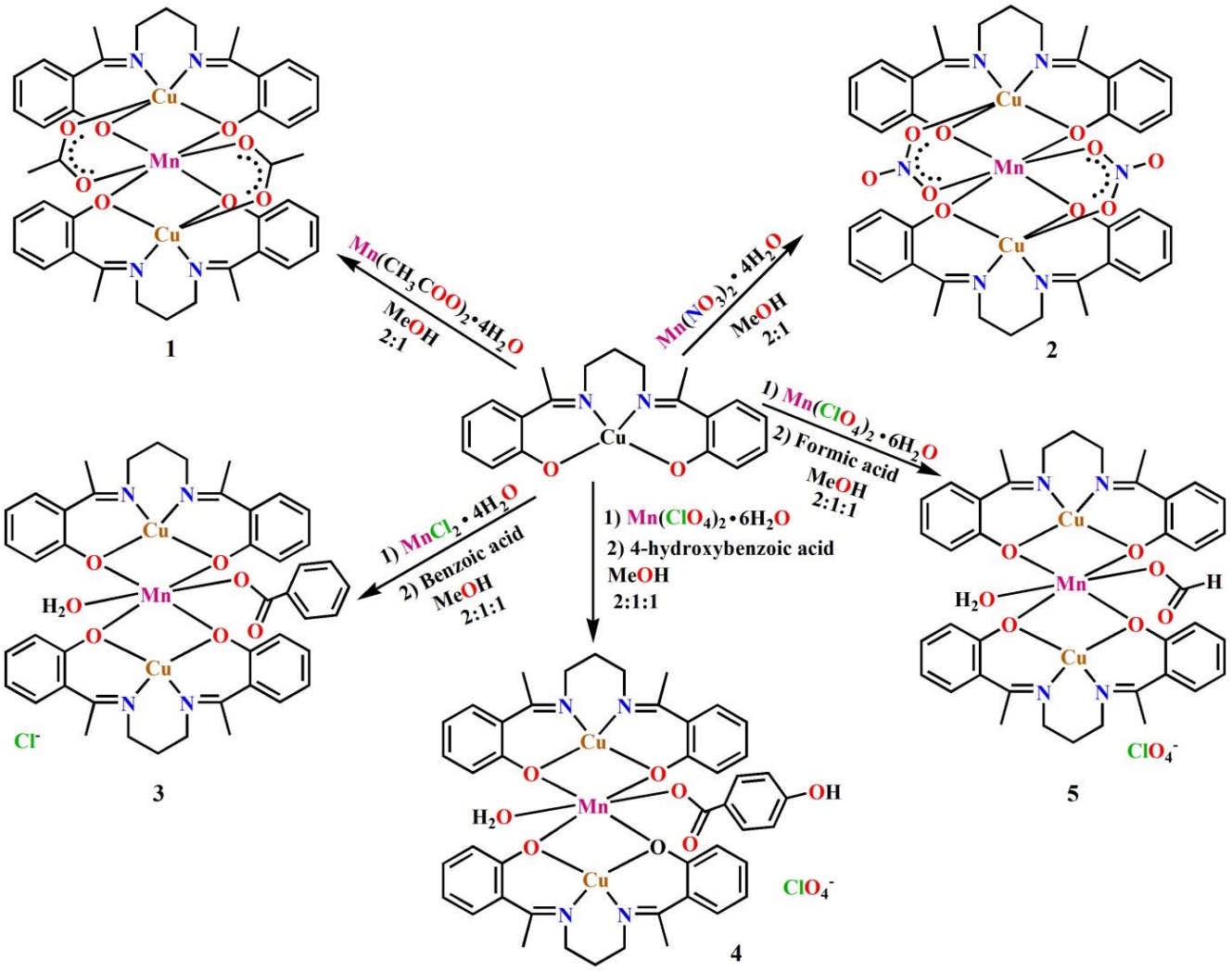

Scheme 1. Syntheses of complexes **1**–**5**.

IR spectra of complexes 1–5

All five complexes show the characteristic stretching vibrations for the azomethine (C=N) group around 1600 cm^{-1}.[18] A sharp peak at 1293 cm^{-1} appears due to the presence of nitrate ion in complex **2**.[19] Two sharp peaks at around 1540 cm^{-1} and 1398 cm^{-1} appear for the symmetric and asymmetric stretching for COO^{-} in complexes **1**, **3**, **4** and **5**.[18a] Moreover, complexes **4** and **5** display a couple of strong intensity band *at ca*. 1101 and 1094 cm^{-1} respectively, confirming the presence of ionic perchlorate[18b] in them. The IR spectral data for the complexes for the complexes are given in the supporting information (Fig. S1−S5, ESI respectively).

Description of the structures

All five structures were found to contain two CuL metalloligands that are bridged by a manganese atom to provide a $MnCu_2L_2$ core. In **1** and **2**, the Mn atom occupied a centre of symmetry in an ordered structure. In **3**, the central Mn atom was imposed on a two-fold axis with a disordered six-coordinate environment. In **4** and **5**, no crystallographic symmetry was imposed on the structures.

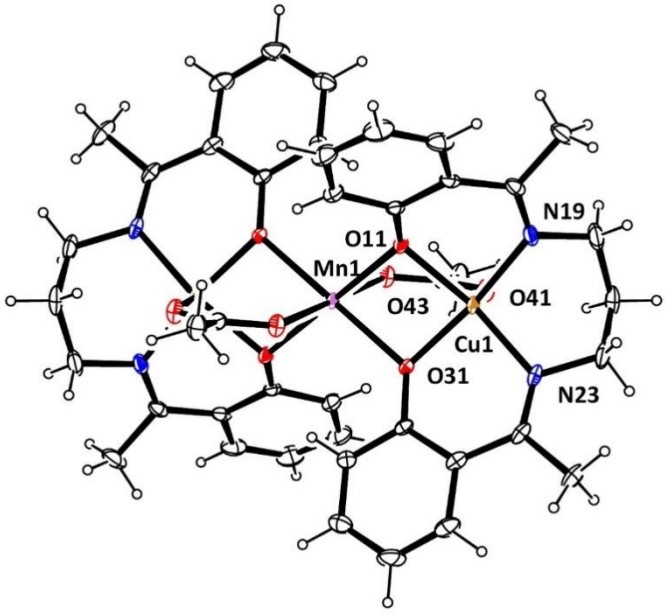

Fig. 1. The structure of **1** with ellipsoids at 20% probability. The Mn atom occupies a centre of symmetry.

The structure of **1** is shown in Fig. 1 with dimensions in Table S1, ESI and contains two metalloligands which are bridged by a Mn atom occupying a centre of symmetry. In the metalloligands the copper atoms are bonded to the O_2N_2 donor atoms of the ligand with distances to O 1.976(2), 1.924(2) Å and to N 1.977(2), 2.001(2) Å. Here the Mn atom bridges the two metalloligands by bonding to the four oxygen atoms at distances of 2.195(2), 2.199(2) Å in an equatorial plane. A second oxygen atom O(41)

of these anions is bonded to the metalloligands *via* the copper atom with Cu-O(41), 2.218(2) Å, thus completing a five-coordinate square pyramidal arrangement around the copper atom. The four donor atoms in the equatorial plane around the metal show an r.m.s. deviation of 0.093 Å with the copper atom 0.238(1) Å from the plane in the direction of the axial atom O(41). The Mn atom is six-co-ordinate with an octahedral geometry in which two monodentate acetate anions occupy axial positions via O(43) at distances of 2.127(2) Å.

There are two independent molecules in the structure of **2** called A and B with similar structures as shown in Fig. 2. As in **1**, the structures contain the two metalloligands bridged by a manganese atom occupying a centre of symmetry. Here the anion is nitrate. Also the nitrate bridges the copper and manganese atoms, with distances Mn(1)-O(43) 2.196(4), Cu(1)-O(41) 2.414(5) Å in 2A and 2.192(4), 2.465(5) Å in 2B.

The dimensions involving the metals with the macrocycle are as expected (Table S1, ESI). The copper atoms have square pyramidal environments with the metal atoms 0.114(2), 0.088(2) Å above the equatorial plane in which the four donor atoms show r.m.s. deviations of 0.070, 0.040 Å respectively. The weak axial interaction is consistent with the small deviation of the copper atoms from the plane. There are three solvent methanol molecules in the asymmetric unit, all refined with 50% occupancy. Dimensions of hydrogen bonding interactions in **2** are given in Table S4.

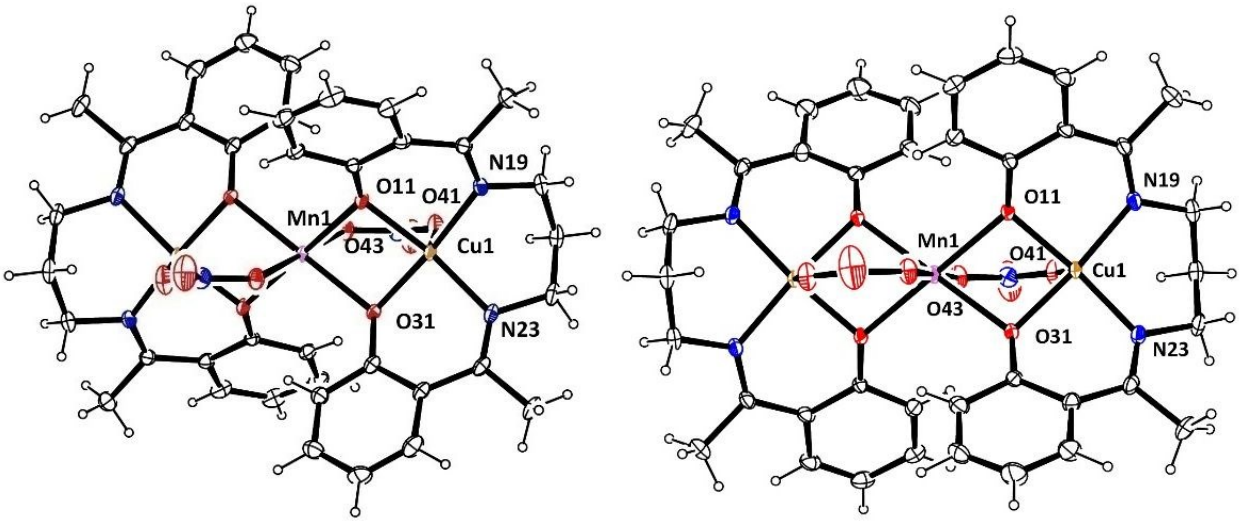

Fig. 2. The structures of **2**A and **2**B with ellipsoids at 20% probability. Solvent methanols are not shown

In the structure of **3**, shown in Fig. 3, which contains a two-fold axis coordination of the two metalloligands remains the same as in complexes **1** and **2** with the copper atoms bonded to the four donor atoms of the macrocycle. However there are no axial atoms and the copper atoms remain four-co-ordinate with square planar environments. Dimensions are listed in Table S2.The copper atoms are

0.039(3) Å from the plane of their four donor atoms which show a r.m.s. deviation of 0.201 Å. Thus the two MnO_2 moieties from the different metallocycles intersect at 74.9(1)° and the MnO_2Cu rings are folded with angles of 32.6(2)° between MnO_2 and CuO_2 moieties. The two CuO_2N_2 planes intersect at 26.2(1)°. The structure of **3** has crystallographically imposed C2 symmetry and as a result the two monodentate ligands, water and benzoate bonded to the manganese atom are disordered. To fit with the imposed symmetry, each monodentate site was refined with 50% occupancy of the two monodentate ligands. The asymmetric unit also contains two water molecules refined with occupancies of 0.5 and 0.25. The Mn-O distances are, Mn-O(11) 2.109(4) Å, Mn-O(31) 2.289(4) Å and Mn-O(41) 2.045(14) Å. The positively charged trinuclear complex is balanced with a chloride which is disordered over two positions, refined with occupancies 0.375 and 0.125.

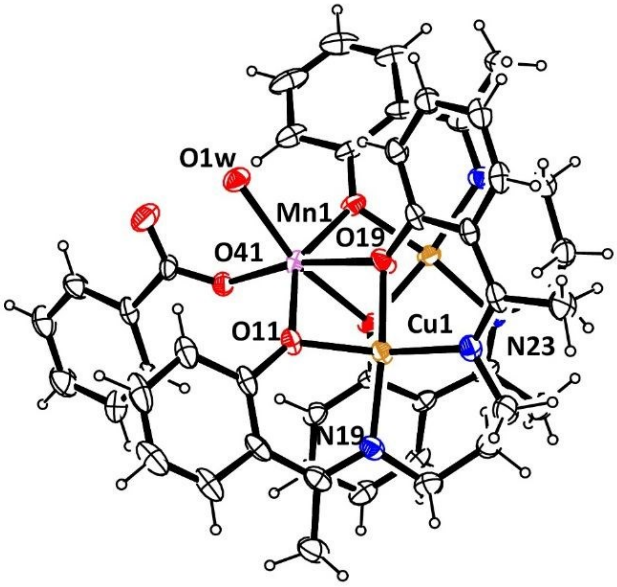

Fig. 3. The structure of one molecule of **3** with ellipsoids at 20 % probability. The hydrogen atoms on the water molecule O1w were not located and are not shown. Only one of the two possible ordered molecules is shown. Disordered chloride and solvent water molecules are also not shown.

By contrast the structure of **4** and **5** are very similar to **3** but contains no crystallographic symmetry and is very different from those of **1** and **2**, as is apparent from Fig. 4.

View Article Online
DOI: 10.1039/D0DT00952K

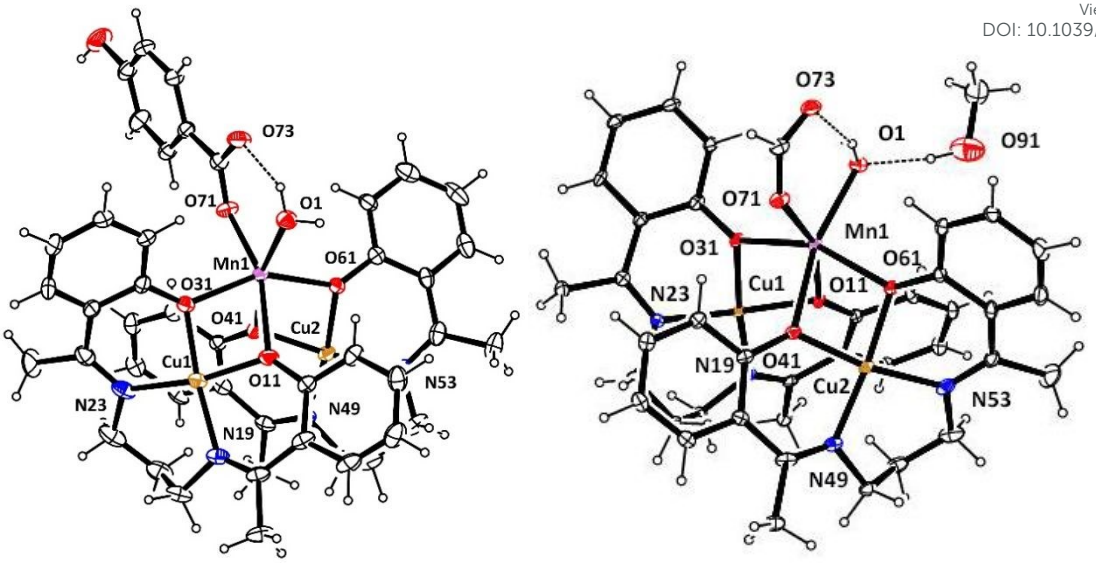

Fig. 4. The structures of **4** (left) and **5** (right) with ellipsoids at 20% probability. In both structures disordered perchlorate ions is not shown nor are solvent water molecules in **4**. Hydrogen bonds are shown as dotted lines.

Similar to **3**, in **4** and **5** the copper atoms are bonded to four O_2N_2 donor atoms of the ligand and have no axial coordination, thus having a square planar geometry. The coordination of the two metalloligands remains the same as in **1** and **2**. The two structures have very similar dimensions which are compared in Table S3. In **4**, the copper atoms are 0.017(3), 0.030(3) Å from the planes with the four donor atoms showing a slight tetrahedral distortion with r.m.s. deviations of 0.104, 0.072 Å. Equivalent dimensions in **5** are 0.041(4), 0.021(4), 0.153, 0.095 Å respectively. The two square planes intersect at 26.9(1), 28.3(2)^o respectively in **4** and **5**. As in **1** and **2**, the four oxygen atoms from the two metalloligands bridge to the manganese but now in a *cis* arrangement in which the angle between the planes Mn(1),O(11),O(31) and Mn(1), O(41), O(61) is 77.9(2), 77.6(2)^o in 4 and 5 respectively compared to the co-planarity found in **1** and **2**. The MnO_2Cu rings are folded with angles of 32.4(2), 32.8(2)^o in **4** and 34.2(2), 50.2(3) in **5** between MnO_2 and CuO_2 moieties. In **4** the six-coordinate octahedral structure of the manganese atom is completed by a water molecule and an oxygen atom from a benzoic acid ligand, in mutually *cis* positions. The Mn-O distances to the oxygen atoms of the metalloligands show significant variations with Mn-O(11) 2.326(6), Mn-O(31) 2.126(6), Mn-O(41) 2.273(5) and Mn-O(61) 2.118(5) Å. The bond lengths involving the monodentate ligands are Mn(1)-O(71) at 2.079(5) Å, and Mn-O(1W) at 2.164(6) Å. In 5 the equivalent dimensions are 2.346(6), 2.119(6), 2.234(6), 2.108(7) Å to the oxygen atoms from the metalloligands and 2.108(7) Å to the formate oxygen O(71) and 2.183(7) Å

to the water molecule O(1). These two trinuclear complexes have a positive change which is balanced by a perchlorate anion which in both structures is disordered and refined with two sets of four oxygen atoms. In **4**, there are in addition six solvent water molecules, all refined with 50% occupancy. The water molecule bonded to the Mn forms donor hydrogen bonds to perchlorate oxygen as well as two of these solvent water molecules. The hydrogen atom of the –OH moiety on the benzoate anion also forms a hydrogen bond to a solvent water molecule. In **5**, there are hydrogen bonds between the unbonded formate oxygen O(73) and the coordinated water molecule O(1) and also between O(1) and a methanol solvent molecule. Dimensions of these hydrogen bonds in **4** and **5** are given in Table S5 and S6 respectively.

It is noticeable from Fig. 4 that the arrangement of the two metalloligands around the manganese atom approximates to C2 symmetry in both structures although the symmetry is necessarily broken by the fact that the two monodentate ligands bonded to Mn are different being a water molecule together with a benzoate in **4** and a formate in **5**.

Magnetic properties

The magnetic properties of complexes **1**, **2**, **3**, **4** and **5** on powdered and pressed samples were investigated in the 2–300 K temperature range and under a field of 0.3 T and plotted as $\chi_M T$ *vs.* *T* plots as shown in Fig. 5. The corresponding magnetization plots are included in ESI, Fig. S6.

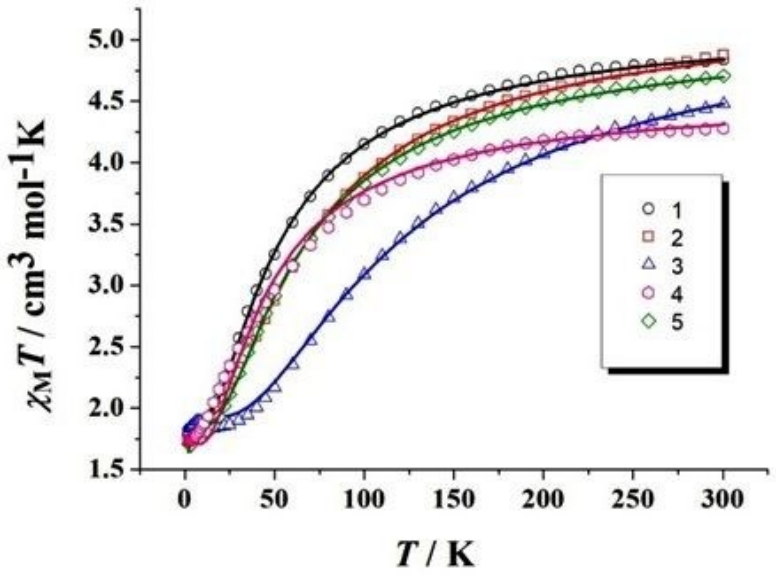

Fig. 5. Representation of $\chi_M T$ as a function of *T* for complexes **1** (black circles), **2** (red squares), **3** (blue triangles), **4** (pink hexagons) and **5** (green rhombs). Solid lines represent the best fit for each product.

Complexes **1–5** are trinuclear Cu(II)–Mn(II)–Cu(II) species, showing an overall antiferromagnetic behavior. The experimental values of $\chi_M T$ at room temperature are given in Table 2; all of them are in good agreement with the theoretical value of 5.125 $cm^3 \cdot mol^{-1} \cdot K$ corresponding to two Cu(II) and one Mn(II) non-interacting cations. All five complexes have a similar magnetic response where the $\chi_M T$ as a function of T curve continuously decays on lowering of temperature tending to values close to 1.75 $cm^3 \cdot mol^{-1} \cdot K$ at 2 K as is expected for a S = 3/2 ground state (1.875 $cm^3 \cdot mol^{-1} \cdot K$) that confirms the antiferromagnetic interaction, Table 2. Slight differences in the shape of the curve are noted for complex **3**, suggesting larger antiferromagnetic interactions.

Table 2. Magnetic parameters of complexes **1–5** extracted from the experimental data and the fitting curves of $\chi_M T$ *vs*. T plots.

Complex	$\chi_M T$/$cm^3 \cdot mol^{-1} \cdot K$(300 K)	$\chi_M T$/$cm^3 \cdot mol^{-1} \cdot K$(2 K)	J_1 /cm^{-1}	g
1	5.06	1.82	-8.54	2.02
2	5.04	1.75	-11.50	2.10
3	4.48	1.81	-19.83	2.04
4	4.28	1.72	-10.65	2.02
5	4.71	1.71	-10.27	2.05

The Spin-Hamiltonian $H = -2J\,(\hat{S}_{Mn} \cdot \hat{S}_{Cu1} + \hat{S}_{Mn} \cdot \hat{S}_{Cu2})$ in the full temperature range has been used to fit the curves for **1–5** using PHI software.[20] The best fitting parameters, J_1 and global g value for all the complexes are summarized in Table 2.

In the case of the linear complexes **1** and **2**, the bridging between the central Mn(II) cation with the two Cu(II) cations is through the Schiff base ligans (bis-phenoxido bridge) along with a *syn-syn* carboxylate bridge. However, the *syn-syn* carboxylate pathway has negligible influence in the magnetic response because the axial position of the Cu(II) cations involves a non-magnetic orbital (d_{z2}) that does not allow magnetic coupling. Complexes **3**, **4** and **5** show a similar structure with

the bis-phenoxido bridges in *cis* configuration and without additional carboxylato bridges. The magnitude of *J* for **3** is slightly larger, evidencing a stronger antiferromagnetic interaction.

The magneto-structural corrections in these kind of complexes with a bis(phenoxido) bridge between Cu(II)–Mn(II) have been previously studied by us and it was found that the main contributive factor to the super-exchange interaction in these type of complexes is the Cu(II)–O–Mn(II) angle.[21] The reported complexes in the present text also confirm that a greater antiferromagnetic coupling is associated with larger Cu(II)–O–Mn(II) angles (Fig. 5). However, looking at the representation of the magneto-structural correlation in Fig. 7, it is clear that relation between *J* and the structural parameters is a multifactor problem and parameters other than the bridging angle should also be taken into account for such correlations. In the case of complexes **1** and **2**, there is a carboxylate bridge connecting the paramagnetic centers. This kind of bridge can present counter-complementarity with the oxo bridges, and though weak, may decrease the magnetic coupling. Another factor that could affect the magnetic correlations is the shape: some molecules are linear (where the magnetic coupling is exclusively through the d_{x2-y2} orbital) while others are folded (in these cases communicating the magnetic exchange trough the d_{x2-y2} orbital and the perpendicular d_{z2} orbital). Finally, the differences in the electronegativity of the groups coordinated to manganese, the bond distances, the dihedral angles or the geometry around the metal ions (in particular the square-planar to tetrahedral distortion for the Cu(II) cations) contribute to the deviations from the single-factor magnetic correlation. The attempts to correlate the magnetic coupling with two parameters such as the bond angle/ring torsion or any other pair of structural parameters, do not improve unequivocally the correlation.

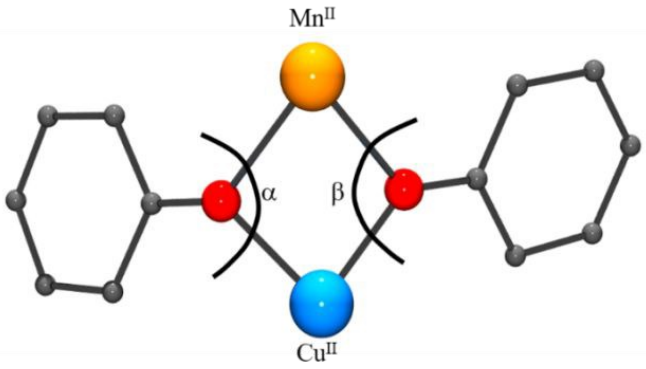

Fig. 6. Representation of the bis(phenoxido) bridge in M(II)–O–Cu(II) complexes. While all the reported complexes give the value of *J* supposing a single exchange pathway, α and β angles have been taken as a mean.

View Article Online
DOI: 10.1039/D0DT00952K

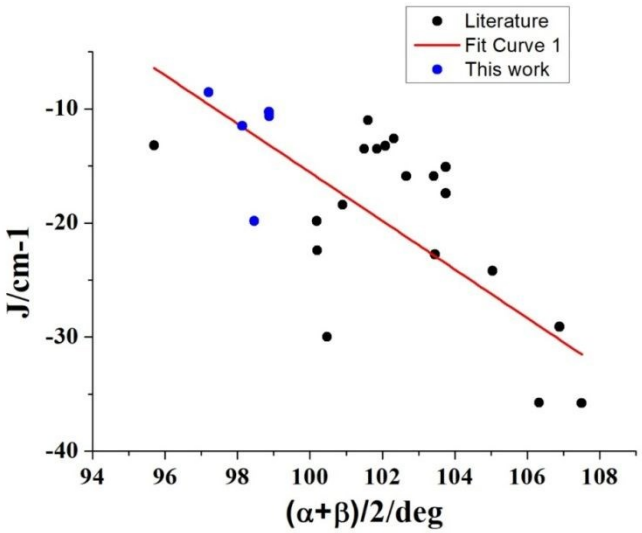

Fig. 7. Dependence of the reported *J* values (considering Spin-Hamiltonian, $H=-2J\cdot S_1S_2$) with the Mn(II)–O–Cu(II) angle. Black spots represent the previously reported complexes found in the literature which follow a good magnetostructural correlation, blue spots correspond to the compounds in this work (Table S7, ESI).

Electrochemistry

Cyclic voltammograms (CVs) of the metalloligand, CuL, and complexes **1**−**5** were recorded in acetontrile solution at a scan rate of 100 mV s^{-1} with respect to an Ag/AgCl electrode. Metalloligand CuL shows a reversible red-ox process due to Cu(II)/Cu(I) couple at the electrode surface with E_c = −1.15 V and E_a = −1.04 V (Fig. S7 (left)). The peak separation value $\Delta E_{pc} = E_c - E_a$ is −0.11 V and I_c/I_a =1.09. However, cyclic voltamograms of complexes **1**−**5** show prominent peaks at E_c^1 = − 0.77, E_c^2 = −1.03 V for **1,** E_c^1 = −0.72, E_c^2 = −1.06 V for **2**, E_c^1 = −0.75, E_c^2 = −1.02 V for **3**, E_c^1 = −0.75, E_c^2 = −1.14 V for **4** and E_c^1 = −0.76, E_c^2 = − 1.05 V for **5,** respectively (Fig. S7 (right))**.** It can be assumed that the trinuclear complexes undergo partial dissociation in acetonitrile solution and in this process of reduction of Cu(II) to Cu(I), the first peak E_c^1 arises due to the undissociated trinuclear species while the second peak, E_c^2, due to the free metalloligand. Such partial dissociation and appearance of two peaks in CV of such complexes were also observed earlier[22]. It is noticeable that in the trinuclear species, the reduction of Cu(II) to Cu(I) takes place at less negative potential compared to CuL as coordination of the metalloligand to Mn(II) makes Cu(II) more susceptible to reduction.

Catechol Oxidase Studies and Kinetics.

The catecholase like activity of complexes **1**−**5** for areal oxidation of 3,5-di-*tert*-butylcatechol (3,5-DTBC) to 3,5-di-*tert*-butylquinone (3,5-DTBQ)[23] was studied in acetonitrile medium under open atmosphere. The oxidation of 3,5-DTBC produces 3,5-DTBQ according to the reaction shown in Scheme 2.

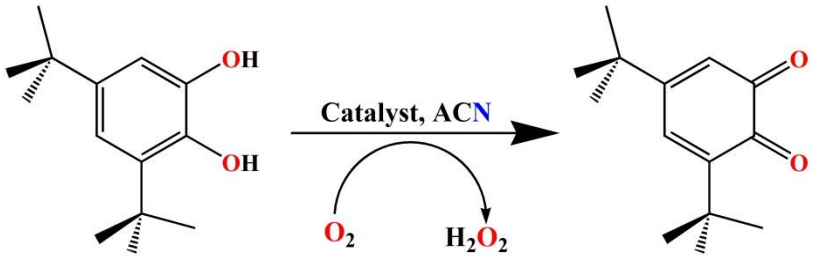

Scheme 2. Catalytic Oxidation of 3,5-DTBC to 3,5-DTBQ in acetonitrile solution (ACN).

In order to carry out the experiment, 2 x 10^{-5} M acetonitrile solutions of each of the complexes, **1**−**5** was mixed with 2 x 10^{-3} M solutions of 3,5-DTBC at room temperature in equal volumes and the progress of the reaction was studied by performing absorbance *versus* wavelength scan of the mixtures at regular intervals of 3 min for half an hour (wave scan). The gradual increase in the absorption maxima near 398 nm is observed due to formation of 3,5-DTBQ[24] for complexes **1**, **3**, **4** and **5**. Complex **2** shows no increase in absorbance maxima for over 30 min, indicating that it is inactive towards catechol oxidase activity. The absorbance *vs.* wavelength plot of complexes **1** (left) and **3** (right) are shown in Fig. 8 and those of complexes **2**, **4** and **5** are shown in the supporting information (Fig.s S8 and S9 respectively).

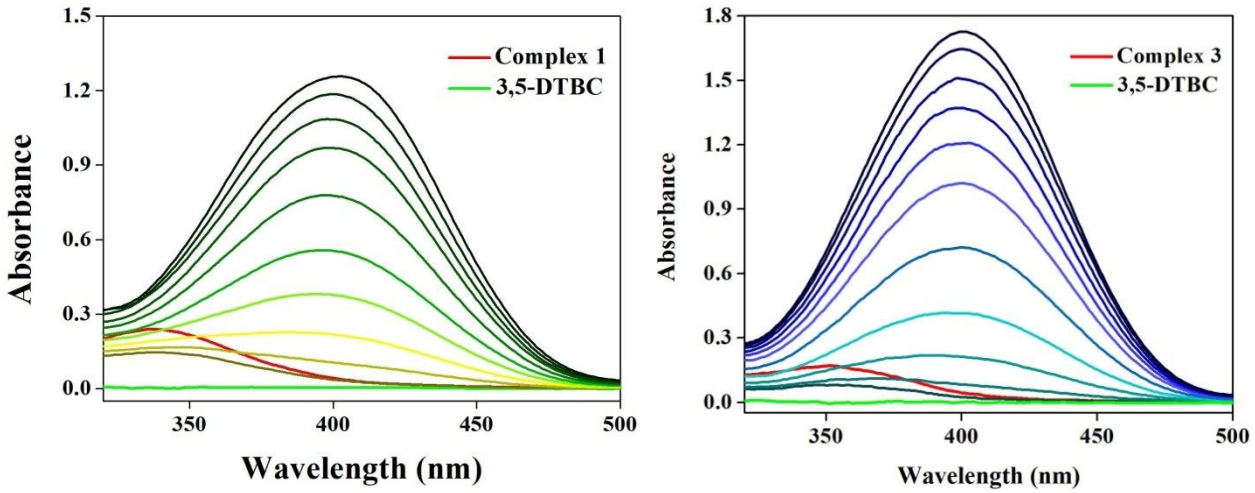

Fig. 8. Increase of the quinone band at around 398 nm after mixing equal volumes of acetonitrile solutions of 2 x 10^{-3} M 3,5-DTBC and 2 x 10^{-5} M complex **1** (left) and complex **3** (right), respectively. The spectra were recorded at 3 min interval for 30 min.

The kinetics of this oxidation reaction of 3,5-DTBC to 3,5-DTBQ in the presence of complexes **1**, **3**, **4** and **5** were determined following initial rate method by measuring the growth of the quinone band at 398 nm as a function of time (timescan). The dependence of oxidation rate on the substrate concentration was studied by mixing equal volumes of 1 × 10^{-5} M solution of the complexes with various concentrations of the substrate (5 × 10^{-5} M, 1 × 10^{-4} M, 3 × 10^{-4} M, 1 × 10^{-3} M, 1.2 × 10^{-3} M, 2 × 10^{-3} M, 4 × 10^{-3} M, 6 × 10^{-3} M, 8 × 10^{-3} M, 1 × 10^{-2} M and 1.2 × 10^{-2} M). For all these measurements, the corresponding solution of substrate without catalyst was taken as reference. The initial rate was determined from the slope of the absorbance *vs*. time plot taking the data of first 10 min and considering the molar extinction coefficient of quinone (3,5-DTBQ) as 1630 M^{-1} cm^{-1}.[25] The rate constant *vs*. concentration of 3,5-DTBC data were then analyzed on the basis of the Michaelis–Menten approach of enzymatic kinetics to obtain the Lineweaver–Burk (double reciprocal) plot as well as the values of various kinetic parameters such as V_{max}, K_M, and K_{cat}. The curves of both the observed rate *vs*. [substrate] and the Lineweaver-Burk plot for complexes **1** and **3** are depicted in Fig. 9 and the same for complexes **4** and **5** are shown in the supporting information (Fig.s S10 and S11 respectively).

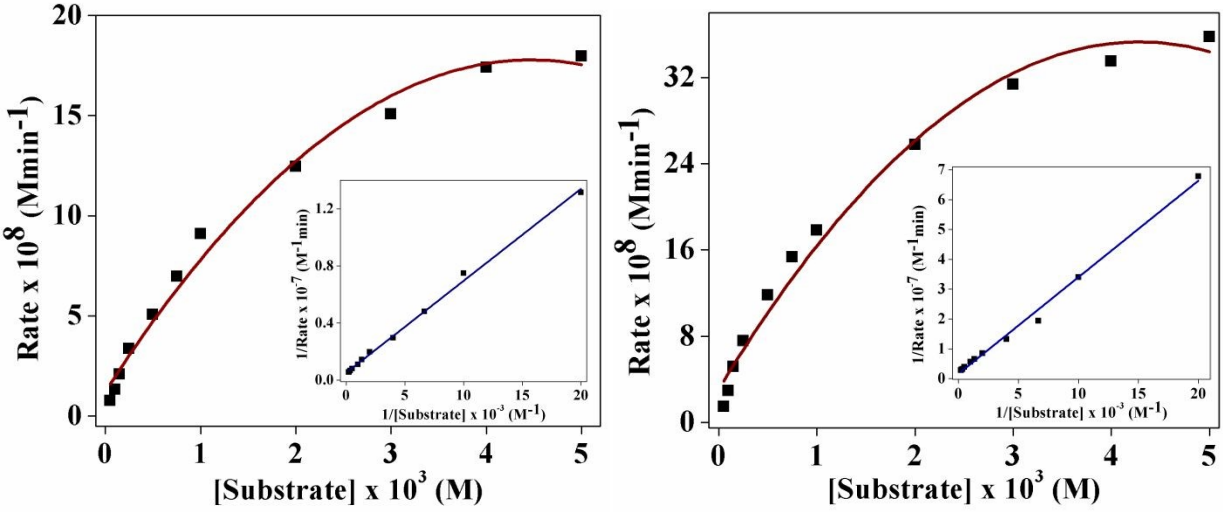

Fig. 9. Plots of rate *vs.* substrate concentration for complexes **1** (left) and **3** (right).The insets show the corresponding Lineweaver-Burk plot.

The turnover number, K_{cat} (in h^{-1}) of this catechol oxidase reaction is calculated to be 139 h^{-1} for **1**, 439 h^{-1} for **3**, 348 h^{-1} for **4** and 730 h^{-1} for **5**. The kinetic parameters of the complexes are given in Table 3.

Table 3. Values of parameters K_m, V_{max} and K_{cat} obtained from Lineweaver Burk plots.

Complex	K_m	V_{max}	K_{cat}
1	1.24×10^{-3}	1.93×10^{-7}	139 h^{-1}
3	1.97×10^{-3}	6.09×10^{-7}	439 h^{-1}
4	1.56×10^{-3}	4.84×10^{-7}	348 h^{-1}
5	1.68×10^{-3}	1.01×10^{-6}	730 h^{-1}

ESI-Mass Spectrometric Study.

To suggest a probable mechanism for the catechol oxidase activity of complexes **1**, **3**, **4** and **5** the ESI-mass spectra of the complexes (Fig.s S12–S16, ESI) and 1:1 (*v/v*) mixture of complex and 3,5-DTBC (1:10^2 molar ratio) were recorded in acetonitrile medium (Fig.s S17–S20, ESI). The mass spectra of complexes **1**, **3**, **4** and **5** show base peak at *m/z* = 372.07 (cald. = 372.09) which is assignable to $[(CuL) + H]^+$. Prominent peaks at *m/z* = 394.07, 743.16 and 765.16 are common for all four complexes and can be assigned to $[(CuL) + Na]^+$ (cald. = 394.07), $[(CuL)_2 + H]^+$ (cald. = 743.14), $[(CuL)_2 + Na]^+$ (cald. = 765.15) respectively. For complex **1**, a peak at *m/z* = 527.08 (cald. = 527.06) is seen which can be attributed to $[(CuL)Mn(CH_3COO) + CH_3CN]^+$. For **3**, the peak at *m/z* = 565.06 (cald. = 565.06) is assigned to $[(CuL)Mn(C_6H_5COO)(H_2O)]^+$. In **4**, a peak for $[(CuL)Mn((p\text{-}OH)C_6H_5COO)(H_2O)]^+$ is found at *m/z* = 581.05 (cald. = 581.05) and for complex **5** the peak at *m/z* = 489.09 (cald. = 489.09) is assigned to $[(CuL)Mn(HCOO)(H_2O)]^+$.

Complexes **1**, **3**, **4** and **5** were then mixed separately with 3,5-DTBC in the molar ratio of 1 : 10^2 and after 5 min, again the spectra were recorded. For all four cases, the base peak was found at *m/z* = 372.07 (cald. = 372.09) which was assigned to $[(CuL) + H]^+$. Other common peaks are found at *m/z* = 648.16, 649.16 and 243.14 which may be assigned to $[(CuL)Mn(3,5\text{-}DTBC) + H]^+$ (cald. = 648.16), $[(Cu(I)L)Mn(3,5\text{-}H_2DTBC)]^+$ (cald. = 649.16) and $[3,5\text{-}DTBQ + Na]^+$ (cald. = 243.14) respectively. In the ESI-mass spectra of complex **1**, the peaks at *m/z* = 609.10 and 467.04

can be assigned to $[(CuL)Mn(CH_3COO) + 3CH_3CN]^+$ (cald. = 609.12) and $[(Cu(I)L)Mn + CH_3CN]^+$ (cald. = 467.04), respectively. The mass spectra of complex **3** shows peaks at *m/z* = 565.06, 768.20 and 444.83 for $[(CuL)Mn(C_6H_5COO)(H_2O)]^+$ (cald. = 565.06), $[(CuL)Mn(C_6H_5COO)(3,5\text{-DTBC}) + H]^+$ (cald. = 768.20) and $[(Cu(I)L)Mn(H_2O)]^+$ (cald. = 444.83), respectively. For complex **4** peaks at *m/z* = 622.09 and 444.83 may be assigned to $[(CuL)Mn((p\text{-OH})C_6H_5COO)(H_2O) + CH_3CN]^+$ (cald. = 622.09) and $[(Cu(I)L)Mn(H_2O)]^+$ (cald. = 444.83), respectively. Similarly for **5,** peaks at *m/z* = 489.02 and 444.83 are assignable to $[(CuL)Mn(HCOO)(H_2O)]^+$ (cald. = 489.03) and $[(Cu(I)L)Mn(H_2O)]^+$ (cald. = 444.83), respectively.

Mechanistic Insight for Complexes 1, 3, 4 and 5

The mechanistic studies of copper based model complexes for catechol oxidase type activities reveal that there are two routes for conversion of 3,5-DTBC to 3,5-DTBQ. The first mechanism involves formation of a dicopper(II) catecholate intermediate where the dicopper(II) species stoichiometrically oxidizes the catecholic substrate to one molecule of quinone and itself reduces to a dicopper(I) species. This dicopper(I) species reacts with an oxygen molecule to generate a peroxo dicopper(II) adduct, which then oxidizes a second molecule of the substrate to quinone; water is formed as a byproduct in this four electron reduction process.[26] The second mechanism is proposed to proceed through formation of a copper(I) semiquinonate radical[27] intermediate which reacts with a dioxygen molecule, reducing it to H_2O_2 by a two electron reduction[28] and the Cu(I) in the radical is oxidized to Cu(II). A quinone molecule is produced in the process. In order to get an idea of which pathway is followed, we were interested to know if H_2O_2 is released. The estimation of H_2O_2 shows that after 1 h of oxidation, 92%, 94%, 91% and 95% of H_2O_2 is generated with respect to the formation of 3,5-DTBQ for **1**, **3**, **4** and **5**, respectively as shown in Fig. S21 (ESI). The results indicate that almost equimolar amount of hydrogen peroxide is formed with respect to 3,5-DTBQ.

Based on the ESI-mass spectra, we propose a probable mechanistic pathway for the oxidation reaction catalyzed by complexes **1**, **3**, **4** and **5**. ESI-mass spectra reveals that complexes **1**, **3**, **4** and **5** generate active monopositive species, $[(CuL)Mn(CH_3COO)]^+$, $[(CuL)Mn(C_6H_5COO)(H_2O)]^+$, $[(CuL)Mn((p\text{-OH})C_6H_5COO)(H_2O)]^+$ and $[(CuL)Mn(HCOO)(H_2O)]^+$, respectively in the solution.

The X-ray crystallographic studies reveal that complexes **3**, **4** and **5** contain a water molecule coordinated to the central metal atom, Mn(II) but in **1** no such solvent molecule is present. As a

result a subtle difference is proposed in the mechanistic pathways of complexes **1** and **3**, **4** and **5**. Schematic representation of catalysis of complex **3** is shown in Scheme 3 and that of **1**, **4** and **5** are attached in the supporting information (Scheme S1, S2 and S3, respectively). In the case of complex **1**, the acetate ion of cationic species, $[(CuL)Mn(CH_3COO)]^+$ is replaced by a mononegative catecholate molecule, forming an intermediate species, $[(CuL)Mn(3,5\text{-}HDTBC)]^+$. This species further loses another hydrogen ion to form a semiquinonate radical complex, $[(CuL)Mn(3,5\text{-}DTBC)]^+$ as evident from the mass spectra. However, in the case of complex **3**, the active cationic species first loses the labile water molecule and reacts with singly deprotonated 3,5-DTBC to form an intermediate complex $[(CuL)Mn(C_6H_5COO)(3,5\text{-}HDTBC)]^+$. In the next step, the benzoate ion is lost and semiquinonate radical, $[(CuL)Mn(3,5\text{-}DTBQ)]^+$ similar to complex **1** is formed. With formation of the semiquinonate radical complex, O_2 is reduced to H_2O_2. Following this, the semiquinone is oxidized to quinone and is eliminated from the metal center with the reduction of Cu(II) to Cu(I) forming a monocationic species $[(Cu(I)L)Mn]^+$ for **1** and $[(Cu(I)L)Mn(H_2O)]^+$ for **3**, when a water molecule binds to the remaining species of **3**. Then another 3,5-H_2DTBC molecule coordinates to this species to form $[(Cu(I)L)Mn(3,5\text{-}H_2DTBC)]^+$. Finally, the Cu(I) center of the dinuclear active species is oxidized to Cu(II) by aerial O_2 and the active species $[(CuL)Mn(3,5\text{-}DTBC)]^+$ is regenerated, with the formation of H_2O_2 as byproduct as shown in Scheme 3.

View Article Online
DOI: 10.1039/D0DT00952K

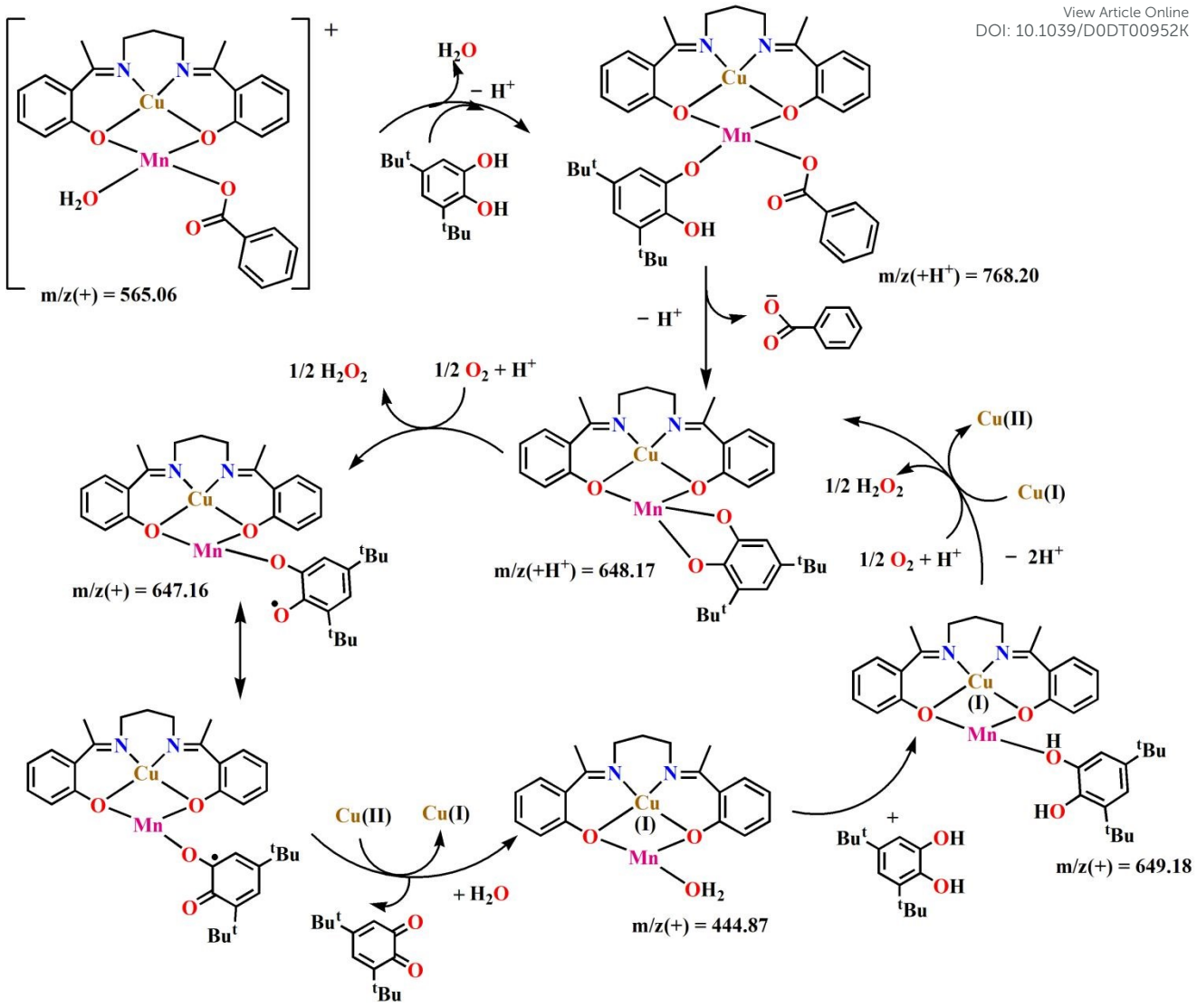

Scheme 3. Proposed Mechanism for Catalytic Oxidation of 3,5-DTBC to 3,5-DTBQ by Complex **3**.

Structure−Activity Correlation for the Catalytic Activity

Literature reveals that various homometallic Cu(II), Ni(II), Mn(II/III) and Fe(II/III) complexes can mimic the catechol oxidase activity but in most cases the efficiency is much lower compared to the native enzyme.[29] However, recently it has been shown that the efficiency of this reaction can be increased many fold by using heterometallic complexes as catalyst presumably due to cooperative activity of two different metal ions. For example, in the Cu–Mn complexes, that showed very high catalytic activity, the Mn(II) ion seems to do the job of binding with the substrate while Cu(II) participate in the redox process.[30] It has also been noted that a labile solvent molecule, coordinated to the Mn centre is the common feature of the complexes showing the enhanced catalytic efficiency of these complexes. [31] The reason behind this phenomenon is that the

substrate can easily replace the labile solvent molecule and gets bonded with the catalyst. Among the present complexes, **3**, **4** and **5** have a water molecule coordinated to Mn(II) and hence show very high catecholase-like activity as expected. However, the k_{cat} value of **5** is significantly higher compared to **3** and **4**. This may be attributed to the lower steric demand of the formate ion compared to benzoate/*p*-hydroxybenzoate that facilitates the coordination of the substrate to the complex. On the other hand, neither **1** nor **2** contain a coordinated solvent molecule to its Mn atom and these two compounds are isostructural. Nevertheless, complex **1** shows significant catalytic activity while **2** is inert towards the catalytic reaction. This difference in behaviour probably lies in the difference of the basicity of the acetate and the nitrate ions. Acetate being the stronger base, can accept a proton from catechol molecule and gets detached from metal ions to make the way for substrate-catalyst binding. The nitrate ion which has considerably low basicity does not accept a proton easily and thus cannot be replaced by the catechol molecule in the metal centre. Hence complex **2** is inactive toward the catalytic reaction. To investigate if acetate ion can activate complex **2**, we mixed a 2 x 10^{-5} M acetonitrile solution of complex **2** with equal volume of 4 x 10^{-5} M solution of sodium acetate in MeOH-AcCN mixture (1:10 *v/v*). The resulting solution was then mixed with 2 x 10^{-3} M acetonitrile solution of 3,5-DTBC in equal volumes and absorbance *vs.* wavelength scan was performed (Fig. S22, ESI). An increase in absorption maxima near 398 nm with time clearly indicates that acetate ion indeed makes complex **2** active towards oxidation of catechol. Another point to be noted here is that although the reduction potential of Cu(II) to Cu(I) in all the complexes (**1**–**5**) are very close, complexes **1**, **3**, **4** and **5** are catalytically active with different efficiencies while **2** is catalytically inactive. This implies that coordination environment and coligands around the manganese centre and not the ease of reduction of copper is crucial for catalytic activity/efficiency of such heterometallic complexes.

Conclusion

In this current work, we have synthesized five Cu(II)-Mn(II) complexes of an N_2O_2 donor ligand varying the anionic co-ligands. Among the complexes, **1** and **2** contain only one type of anions, bridging bidentate acetate and nitrate, respectively, as during synthesis only these ions are available for balancing the charge of the respective complexes. On the other hand, each of complexes **3**−**5** which have been prepared by a slightly different procedure, contains two different anions: one monodentate carboxylate and one uncoordinated ClO_4^-/ Cl^- along with a coordinated solvent molecule to the Mn(II) centre. Thus, we have shown here that by the judicious choice of the synthetic procedure, the structures and composition of the resulting complexes can be

monitored. Among the complexes, **3**, **4** and **5** exhibit high catalytic activity for the oxidation of 3,5-di-*tert*-butylcatechol to 3,5-di-*tert*-butylquinone. This is not surprising as it has been observed previously that if a solvent molecule is coordinated to the Mn(II) in such a heterometallic complex, it shows high catalytic activity. However, comparing their K_{cat} values, we have shown here for the first time that catalytic efficiency of such complexes can be related to the steric demand of the anionic co-ligand present in them, as complex **5**, containing the least steric demanding formate ion shows considerably higher efficiency than **3** or **4**. We have also shown here for the first time that basicity of the anionic co-ligands can be important for their catalytic activity as between the isostructural complexes, **1** and **2**, only **1**, containing acetate ion with higher basicity than the nitrate ion in **2** is responsive towards the catalytic process. The variable temperature magnetic study of the complexes confirms intra-molecular antiferromagnetic coupling between Cu(II) and Mn(II) through the phenoxido bridges and larger is the Cu(II)−O−Mn(II) angle greater is the magnitude of antiferromagnetic coupling. In short, the present study reveals that (i) a solvent molecule required for high catalytic activity can be introduced to the metal complex by modifying the synthetic method and (ii) the steric requirements and the basicity of the anionic coligands for this type of heterometallic complexes can be very important for their catalytic efficiency. Thus this study is expected to help in designing the highly efficient catalysts for such oxidase reactions by judicious selection of co-anions and synthetic procedure.

Supporting Information (see footnote on the first page of this article):

IR spectrum of complexes **1**−**5**, magnetization of **1**–**5**, UV-vis spectra of complexes **2**, **3** and **5** with 3,5-DTBC, Lineweaver-Burk plot of complexes **4** and **5**, ESI-mass spectra of complexes **1**−**5**, complexes **1**, **3**, **4** and **5** after addition of 3,5-DTBC. UV-vis spectra of H_2O_2 emission, mechanistic pathways of catalytic reaction for **1**, **4** and **5**, tables of bond parameters of **1**–**5**, tables of hydrogen bond for **2**, **4** and **5**, a comparative table of *J* values. CCDC 1990112 (**1**), 1990113 (**2**), 1990114 (**3**), 1990115 (**4**) and 1990116 (**5**) contain the supplementary crystallographic data for this paper. These data can be obtained free of charge from The Cambridge Crystallographic Data Centre *via* www.ccdc.cam.ac.uk/data_request/cif.

Acknowledgements

A. G. thanks University Grants Commission (UGC), New Delhi for funding the CAS-V, Department of Chemistry, and University of Calcutta. S. D. and P. B. thank the University Grants

Commission (UGC), New Delhi, for Senior Research Fellowship [Sr. No.- 2121410161, Ref No.- 21/12/2014(II)EU-V] and [F. No. 16-9(June 2017)/2018(NET/CSIR), Ref. No.:240/(CSIR-UGC NET JUNE 2017)] respectively. J. M. thanks CICYT, Project CTQ2018-094031-B-100.

References

1 (a) C. T. Lyons and T. D. P. Stack, *Coord. Chem. Rev.*, 2013, **257**, 528 − 540; (b) Z. Chen, H. Morimoto, S. Matsunaga and M. Shibasaki, *J. Am. Chem. Soc.*, 2008, **130**, 2170−2171; (c) M. Andruh, *Chem.Commun*. 2011, **47**, 3025−3042; (d) K. Liu, W. Shi and P. Cheng, *Coord. Chem. Rev.*, 2015, **289**, 74−122; (e) M. Keener, M. Peterson, R. H. Sánchez, V. F. Oswald, G. Wu and G. Ménard, *Chem.Eur. J.*, 2017, **23**, 11479 − 11484; (f) S. Handa, V. Gnanadesikan, S. Matsunaga and M. Shibasaki, *J. Am. Chem. Soc.*, 2010, **132**, 4925−4934.

2 (a) T. J. Boyle, J. M. Sears, J. A. Greathouse, D. Perales, R. Cramer, O. Staples, A. L. Rheingold, E. N. Coker, T. M. Roper and R. A. Kemp, *Inorg.Chem.*, 2018, **57**, 2402−2415; (b) R. Gheorghe, P. Cucos, M. Andruh, J.-P. Costes, B. Donnadieu and S. Shova, *Chem.- Eur. J.*, 2006, **12**, 187−203; (c) S. Roy, A. Bhattacharyya, S. Purkait, A. Bauzá, A. Frontera, S. Chattopadhyay, *DaltonTrans.*, 2016, **45**, 15048−15059.

3 (a) L. Zhao, J. Wu, H. Ke and J. Tang, *Inorg. Chem.*, 2014, **53**, 3519−3525; (b) G. Brunet, F. Habib, I. Korobkov and M. Murugesu, *Inorg. Chem.*, 2015, **54**, 6195−6202; (c) M. Alexandru, D. Visinescu, M. Andruh, N. Marino, D. Armentano, J. Cano, F. Lloret and M. Julve, *Chem. -Eur. J.*, 2015, **21**, 5429 − 5446; (d) Y. Ida, S. Ghosh, A. Ghosh, H. Nojiri and T. Ishida, *Inorg. Chem.*, 2015, **54**, 9543−9555; (e) A. M. Madalan, N. Avarvari, M. Fourmigue, R. Clerac, L. F. Chibotaru, S. Clima and M. Andruh, *Inorg. Chem.*, 2008, **47**, 940−950.

4 (a) P. Seth and A. Ghosh, *RSC Adv.*, 2013, **3**, 3717–3725; (b) S. Dutta, S. Jana, P. Mahapatra, A. Bauzáb, A. Frontera, and A. Ghosh, *CrystEngComm*, 2018, **20**, 6490-6501; (c) P. Kar, R. Biswas, M. G. B. Drew, A. Frontera and A. Ghosh, *Inorg. Chem.*, 2012, **51**, 1837−1851; (d) P. Mukherjee, M. G. B. Drew, C. J. Gomez-Garcı´a and A. Ghosh, *Inorg. Chem.*, 2009, **48**, 5848–5860.

5 (a) J. Costes, G. Novitchi, S. Shova, F. Dahan, B. Donnadieu and J. Tuchagues, *Inorg. Chem.*, 2004, **43**, 7792 − 7799; (b) S. Maity, A. Mondal, S. Konar and A. Ghosh, *Dalton Trans.*, 2019, **48**, 15170–15183; (c) V. Chandrasekhar, A. Dey, S. Das, M. Rouzières and R. Clérac, *Inorg. Chem.*, 2013, **52**, 2588 − 2598; (d) M. C. Das, S. Xiang, Z. Zhang and B. Chen, *Angew. Chem., Int. Ed.* 2011, **50**, 10510−10520.

6 (a) S. Das, S. Hossain, A. Dey, S. Biswas, J. P. Sutter and V. Chandrasekhar, *Inorg. Chem.*, 2014, **53**, 5020-5028; (b) S. Biswas, S. Das, J. Acharya, V. Kumar, J. V. Leusen, P. Kögerler, J. M. Herrera, E. Colacio and V. Chandrasekhar, *Chem.-Eur.J.*, 2017, **23**, 5154–5170.

7 (a) P. Kar, Y. Ida, T. Ishida and A. Ghosh, *CrystEngComm*, 2013, **15**, 400–410; (b) M. Mondal, S. Giri, P. M. Guha and A. Ghosh, *Dalton Trans.*, 2017, **46**, 697–708; (c) P. Kar, Y. Ida, T. Kanetomo, M. G. B. Drew, T. Ishida and A. Ghosh, *Dalton Trans.*, 2015, **44**, 9795–9804; (d) A. Hazari, S. Giri, C. Diaz and A. Ghosh, *Polyhedron*, 2016, **118**, 70–80.

8 (a) P. Buchwalter, J. Rosé and P. Braunstein, *Chem. Rev.*, 2015, **115**, 28−126; (b) M. H. Pérez-Temprano, J. A. Casares and P. Espinet, *Chem.-Eur.J.*, 2012, **18**, 1864−1884; (c) V. Chandrasekhar, P. Bag, W. Kroener, K. Gieb and P. Müller, *Inorg. Chem.*, 2013, **52**, 13078−13086; (d) K. C. Mondal, A. Sundt, Y. Lan, G. E. Kostakis, O. Waldmann, L. Ungur, L. F. Chibotaru, C. E. Anson and A. K. Powell, *Angew. Chem., Int. Ed.*, 2012, **51**, 7550−7554.

9 (a) B. Chakraborty, S. Bhunya, A. Paul and T. K. Paine, *Inorg. Chem.*, 2014, **53**, 4899−4912; (b) A. Hazari, L. K. Das, R. M. Kadam, A. Bauzá, A. Frontera and A. Ghosh, *Dalton Trans.*, 2015, **44**, 3862−3876; (c) J. Adhikary, A. Chakraborty, S. Dasgupta, S. K. Chattopadhyay, R. Kruszynski, A. Trzesowska-Kruszynska, S. Stepanović, M. Gruden-Pavlović, M. Swart and D. Das, *Dalton Trans.*, 2016, **45**, 12409−12422; (d) C.-T. Yang, M. Vetrichelvan, X. Yang, B. Moubaraki, K. S. Murray, J. J. Vittal, *Dalton Trans.*, 2004, 113−121.

10 (a) C. Mukherjee, T. Weyhermueller, E. Bothe, E. Rentschler and P. Chaudhuri, *Inorg. Chem.*, 2007, **46**, 9895 − 9905; (b) C. E. Barry, P. G. Nayar and T. P. Begley, *J. Am. Chem. Soc.* 1988, **110**, 3333−3334; (c) S. Sagar, S. Sengupta, A. J. Mota, S. K. Chattopadhyay, A. E. Ferao, E. Riviere, W. Lewis and S. Naskar, *Dalton Trans.*, 2017, **46**, 1249−1259; (d) I. A. Koval, P. Gamez, C. Belle, K. Selmeczi and J. Reedijk, *Chem. Soc. Rev.*, 2006, **35**, 814−840; (e) B. Sreenivasulu, F. Zhao, S. Gao, J. J. Vittal, *Eur. J. Inorg. Chem.*, 2006, **2006**, 2656−2670.

11 (a) P. Mahapatra, S. Ghosh, S. Giri, V. Rane, R. Kadam, M. G. B. Drew and A. Ghosh, *Inorg. Chem.*, 2017, **56**, 5105–5121; (b) P. Mahapatra, M. G. B. Drew and A. Ghosh, *Cryst.Growth Des.*, 2017, **17**, 6809–6820.

12 S. Ghosh, S. Giri and A. Ghosh, *Polyhedron*, 2015, **102**, 366–374.

13 (a) A. I. Vogel, (A. Israel). *Wiley,* 1989, 689−690; (b) A. I. Vogel, (A. Israel). *Wiley,* 1989, 714.

View Article Online
DOI: 10.1039/D0DT00952K

14 G. M. Sheldrick, Shelxs97 and Shelxl97, *ActaCryst*., 2008, A64 112–122.

15 G. M. Sheldrick, Shelxs97 *Acta Cryst*., 2008, **A64**, 112; Shelxl2014, *Acta Cryst*., 2015, **C71**, 3–8.

16 (a) M. Mitra, P. Manna, A. Bauzá, P. Ballester, S. K. Seth, S. R. Choudhury, A. Frontera and S. Mukhopadhyay, *J. Phys. Chem. B*, 2014, **118**, 14713 − 14726; (b) A. Neves, L. M. Rossi, A. J. Bortoluzzi, B. Szpoganicz, C. Wiezbicki, E. Schwingel, W. Haase and S. Ostrovsky, *Inorg. Chem*., 2002, **41**, 1788−1794; (c) M. Mirzaei, H. Eshtiagh-Hosseini, A. Bauzá, S. Zarghami, P. Ballester, J. T. Maguee and A. Frontera, *CrystEngComm*, 2014, **16**, 6149−6158.

17 (a) M. G. B. Drew, R. N. Prasad and R. P. Sharma, *Acta Crystallogr*., *Sect. C*, 1985, **41**, 1755−1758; (b) S. Ghosh, S. Biswas, A. Bauzá, M. Barceló-Oliver, A. Frontera and A. Ghosh, *Inorg. Chem.*, 2013, **52**, 7508–7523; (c) K. Iida, I. Oonishi, A. Nakahara and Y. B. Komiyama, *Chem. Soc. Jpn*., 1970, **43**, 2347−2354.

18 (a) S. Dutta, S. Chakraborty, M. G. B. Drew, A. Frontera and A.Ghosh, *Cryst.Growth Des.*, 2019, **19**, 5819–5828; (b) K. Nakamoto, *Wiley-Interscience: New York*, 1978.

19 P. Seth, S. Ghosh, A. Figuerola and A. Ghosh, *Dalton Trans*., 2014, **43**, 990–998.

20 N. F. Chilton, R. P. Anderson, L. D. Turner, A. Soncini and K. S. Murray *J. Comput. Chem*., 2013, **34**, 1164–1175.

21 (a) P. Mahapatra, S. Giri, M. G. B. Drew and A. Ghosh, *Dalton Trans*., 2018, **47**, 3568–3579; (b) K. Nakamoto, *Wiley-Interscience: New York*, 1978; (c) R. Ruiz, F. Lloret, M. Julve and J. Faus, *Inorg.Chimi.Acta*., 1993, **213**, 261–268; (d) L. Bo, Z. Hong, P. Zhi-Quan, S. You, W. Cheng-Gang, Z. Huang.Ping, H. Jing-Dong and Ru-An J.C., *Coord. Chem.*, 2006, **59**, 1271–1280.

22 S. Maity, S. Ghosh and A. Ghosh, *Dalton Trans*., 2019, **48**, 14898–14913.

23 (a) P. Mahapatra, M. G. B. Drew and A. Ghosh, *Dalton Trans.*, 2018, **47**, 13957–13971; (b) J. Mukherjee, and R. Mukherjee, *Inorg. Chim. Acta*, 2002, **337**, 429 − 438; (c) F. Zippel, F. Ahlers, R. Werner, W. Haase, H. F. Nolting and B. Krebs, *Inorg. Chem*., 1996, **35**, 3409−3419.

24 (a) L. K. Das, A. Biswas, J. S. Kinyon, N. S. Dalal, H. Zhou and A. Ghosh, *Inorg. Chem*., 2013, **52**, 11744−11757; (b) A. Hazari, L. K. Das, A. Bauzá, A. Frontera and A. Ghosh, *Dalton Trans*., 2016, **45**, 5730−5740.

25 (a) I. A. Koval, P. Gamez, C. Belle, K. Selmeczi and J. Reedijk, *Chem. Soc. Rev.*, 2006, **35**, 814–840; (b) J. Ackermann, F. Meyer, E. Kaifer and H. Pritzkow, *Chemistry*, 2002, **8**, 247–258.

26 E. Monzani, L. Quinti, A. Perotti, L. Casella, M. Gulotti, L. Randaccio, S. Geremia, G. Nardin, P. Faleschini and G. Tabbi, *Inorg. Chem*., 1998, **37**, 553−562.

27 (a) I. A. Koval, K. Selmeczi, C. Belle, C. Philouze, E. Saint-Aman, I. Gautier-Luneau, A. M. Schuitema, M. V. Vliet, P. Gamez, O. Roubeau, M. Luken, B. Krebs, M. Lutz, A. L. Spek, J. L. Pierre and J. Reedijk, *Chem.- Eur. J*., 2006, **12**, 6138−6150; (b) J. Ackermann, F. Meyer, E. Kaifer and H. Pritzkow, *Chem.- Eur. J*., 2002, **8**, 247 − 258; (c) M. R. Mendoza-Quijano, G. Ferrer-Sueta, M. Floresálamo, N. Aliaga-Alcalde, V. Gómez-Vidales, V. M. Ugalde- Saldívara and L. Gasque, *Dalton Trans*., 2012, **41**, 4985−4997.

28 (a) J. Balla, T. Kiss and R. F. Jameson, *Inorg. Chem*., 1992, **31**, 58−62; (b) K. Selmeczi, M. Reglier, M. Giorgi and G. Speier, *Coord. Chem. Rev*., 2003, **245**, 191−201.

29 (a) S. K. Dey and A. Mukherjee, *Coord. Chem. Rev*., 2016, **310**, 80−115; (b) Y. Thio, X. Yang, J. J. Vittal, *Dalton Trans*., 2014, **43**, 3545−3556; (c) L. I. Simándi, T. M. Simándi, Z. May and G. Besenyei, *Coord. Chem. Rev*., 2003, **245**, 85−93.

30 (a) J. Serrano-Plana, I. Garcia-Bosch, A. Company and M. Costas, *Acc. Chem. Res*., 2015, **48**, 2397−2406; (b) J. Qin, B. Xu, Y. Zhang, D. Yuan and Y. Yao, *Green Chem*., 2016, **18**, 4270−4275; (c) J. A. Garden, P. K. Saini and C. K. Williams, *J. Am. Chem. Soc*., 2015, **137**, 15078−15081; (d) A. M. Chapman, C. Keyworth, M. R. Kember, A. J. J. Lennox and C. K. Williams, *ACS Catal*., 2015, **5**, 1581−1588; (e) S. Behar, P. Gonzalez, P. Agulhon, F. Quignard and D. Świerczyński, *Catal. Today* 2012, **189**, 35−41; (f) S. Yao, C. Herwig, Y. Xiong, A. Company, E. Bill, C. Limberg and M. Driess, *Angew. Chem., Int. Ed*., 2010, **49**, 7054−7058; (g) F. Nahra, Y. Macé, A. Boreux, F. Billard and O. Riant, *Chem*. - *Eur*. *J*., 2014, **20**, 10970−10981.

31 (a) P. Mahapatra, S. Ghosh, S. Giri, V. Rane, R. Kadam, M. G. B. Drew and A. Ghosh, *Inorg. Chem*., 2017, **56**, 5105−5121; (b) S. Dutta, J. Mayans and A. Ghosh, *Dalton Trans.*, 2020, **49**, 1276–1291.

Table of Contents Only

Roles of basicity and steric crowding of anionic coligands in catechol oxidase like activity of Cu(II)-Mn(II) Complexes.

Sabarni Dutta[a], Pradip Bhunia[a], Júlia Mayans[b], Michael G. B. Drew[c], Ashutosh Ghosh[a,*]

Catalytic efficiency of heterometallic Cu(II)-Mn(II) complexes towards oxidation of 3,5-DTBC to 3,5-DTBQ is dependent on the basicity and steric requirement of anionic co-ligands.